

9-3-2001

Measurement of the Top Quark p_T Distribution

T. Affolder

Ernest Orlando Lawrence Berkeley National Laboratory, Berkeley, California

Kenneth A. Bloom

University of Nebraska - Lincoln, kbloom2@unl.edu

Collider Detector at Fermilab Collaboration

Follow this and additional works at: <http://digitalcommons.unl.edu/physicsbloom>



Part of the [Physics Commons](#)

Affolder, T.; Bloom, Kenneth A.; and Fermilab Collaboration, Collider Detector at, "Measurement of the Top Quark p_T Distribution" (2001). *Kenneth Bloom Publications*. 89.

<http://digitalcommons.unl.edu/physicsbloom/89>

This Article is brought to you for free and open access by the Research Papers in Physics and Astronomy at DigitalCommons@University of Nebraska - Lincoln. It has been accepted for inclusion in Kenneth Bloom Publications by an authorized administrator of DigitalCommons@University of Nebraska - Lincoln.

Measurement of the Top Quark p_T Distribution

T. Affolder,²³ H. Akimoto,⁴⁵ A. Akopian,³⁸ M. G. Albrow,¹¹ P. Amaral,⁸ S. R. Amendolia,³⁴ D. Amidei,²⁶ K. Anikeev,²⁴ J. Antos,¹ G. Apollinari,¹¹ T. Arisawa,⁴⁵ T. Asakawa,⁴³ W. Ashmanskas,⁸ F. Afzar,³¹ P. Azzi-Bacchetta,³² N. Bacchetta,³² M. W. Bailey,²⁸ S. Bailey,¹⁶ P. de Barbaro,³⁷ A. Barbaro-Galtieri,²³ V. E. Barnes,³⁶ B. A. Barnett,¹⁹ S. Baroiant,⁵ M. Barone,¹³ G. Bauer,²⁴ F. Bedeschi,³⁴ S. Belforte,⁴² W. H. Bell,¹⁵ G. Bellettini,³⁴ J. Bellinger,⁴⁶ D. Benjamin,¹⁰ J. Bensinger,⁴ A. Beretvas,¹¹ J. P. Berge,¹¹ J. Berryhill,⁸ B. Bevensee,³³ A. Bhatti,³⁸ M. Binkley,¹¹ D. Bisello,³² M. Bishai,¹¹ R. E. Blair,² C. Blocker,⁴ K. Bloom,²⁶ B. Blumenfeld,¹⁹ S. R. Blusk,³⁷ A. Bocci,³⁴ A. Bodek,³⁷ W. Bokhari,³³ G. Bolla,³⁶ Y. Bonushkin,⁶ D. Bortoletto,³⁶ J. Boudreau,³⁵ A. Brandl,²⁸ S. van den Brink,¹⁹ C. Bromberg,²⁷ M. Brozovic,¹⁰ N. Bruner,²⁸ E. Buckley-Geer,¹¹ J. Budagov,⁹ H. S. Budd,³⁷ K. Burkett,¹⁶ G. Busetto,³² A. Byon-Wagner,¹¹ K. L. Byrum,² P. Calafiura,²³ M. Campbell,²⁶ W. Carithers,²³ J. Carlson,²⁶ D. Carlsmith,⁴⁶ W. Caskey,⁵ J. Cassada,³⁷ A. Castro,³² D. Cauz,⁴² A. Cerri,³⁴ A. W. Chan,¹ P. S. Chang,¹ P. T. Chang,¹ J. Chapman,²⁶ C. Chen,³³ Y. C. Chen,¹ M.-T. Cheng,¹ M. Chertok,⁴⁰ G. Chiarelli,³⁴ I. Chirikov-Zorin,⁹ G. Chlachidze,⁹ F. Chlebana,¹¹ L. Christofek,¹⁸ M. L. Chu,¹ Y. S. Chung,³⁷ C. I. Ciobanu,²⁹ A. G. Clark,¹⁴ A. Connolly,²³ J. Conway,³⁹ M. Cordelli,¹³ J. Cranshaw,⁴¹ D. Cronin-Hennessy,¹⁰ R. Cropp,²⁵ R. Culbertson,¹¹ D. Dagenhart,⁴⁴ S. D'Auria,¹⁵ F. DeJongh,¹¹ S. Dell'Agnello,¹³ M. Dell'Orso,³⁴ L. Demortier,³⁸ M. Deninno,³ P. F. Derwent,¹¹ T. Devlin,³⁹ J. R. Dittmann,¹¹ S. Donati,³⁴ J. Done,⁴⁰ T. Dorigo,¹⁶ N. Eddy,¹⁸ K. Einsweiler,²³ J. E. Elias,¹¹ E. Engels, Jr.,³⁵ D. Errede,¹⁸ S. Errede,¹⁸ Q. Fan,³⁷ R. G. Feild,⁴⁷ J. P. Fernandez,¹¹ C. Ferretti,³⁴ R. D. Field,¹² I. Fiori,³ B. Flaughner,¹¹ G. W. Foster,¹¹ M. Franklin,¹⁶ J. Freeman,¹¹ J. Friedman,²⁴ Y. Fukui,²² I. Furic,²⁴ S. Galeotti,³⁴ M. Gallinaro,³⁸ T. Gao,³³ M. Garcia-Sciveres,²³ A. F. Garfinkel,³⁶ P. Gatti,³² C. Gay,⁴⁷ D. W. Gerdes,²⁶ P. Giannetti,³⁴ P. Giromini,¹³ V. Glagolev,⁹ M. Gold,²⁸ J. Goldstein,¹¹ A. Gordon,¹⁶ I. Gorelov,²⁸ A. T. Goshaw,¹⁰ Y. Gotra,³⁵ K. Goulianos,³⁸ C. Green,³⁶ G. Grim,⁵ P. Gris,¹¹ L. Groer,³⁹ C. Grosso-Pilcher,⁸ M. Guenther,³⁶ G. Guillian,²⁶ J. Guimaraes da Costa,¹⁶ R. M. Haas,¹² C. Haber,²³ E. Hafen,²⁴ S. R. Hahn,¹¹ C. Hall,¹⁶ T. Handa,¹⁷ R. Handler,⁴⁶ W. Hao,⁴¹ F. Happacher,¹³ K. Hara,⁴³ A. D. Hardman,³⁶ R. M. Harris,¹¹ F. Hartmann,²⁰ K. Hatakeyama,³⁸ J. Hauser,⁶ J. Heinrich,³³ A. Heiss,²⁰ M. Herndon,¹⁹ C. Hill,⁵ K. D. Hoffman,³⁶ C. Holck,³³ R. Hollebeek,³³ L. Holloway,¹⁸ R. Hughes,²⁹ J. Huston,²⁷ J. Huth,¹⁶ H. Ikeda,⁴³ J. Incandela,¹¹ G. Introzzi,³⁴ J. Iwai,⁴⁵ Y. Iwata,¹⁷ E. James,²⁶ H. Jensen,¹¹ M. Jones,³³ U. Joshi,¹¹ H. Kambara,¹⁴ T. Kamon,⁴⁰ T. Kaneko,⁴³ K. Karr,⁴⁴ H. Kasha,⁴⁷ Y. Kato,³⁰ T. A. Keaffaber,³⁶ K. Kelley,²⁴ M. Kelly,²⁶ R. D. Kennedy,¹¹ R. Kephart,¹¹ D. Khazins,¹⁰ T. Kikuchi,⁴³ B. Kilminster,³⁷ B. J. Kim,²¹ D. H. Kim,²¹ H. S. Kim,¹⁸ M. J. Kim,²¹ S. H. Kim,⁴³ Y. K. Kim,²³ M. Kirby,¹⁰ M. Kirk,⁴ L. Kirsch,⁴ S. Klimenko,¹² P. Koehn,²⁹ A. Königter,²⁰ K. Kondo,⁴⁵ J. Konigsberg,¹² K. Kordas,²⁵ A. Korn,²⁴ A. Korytov,¹² E. Kovacs,² J. Kroll,³³ M. Kruse,³⁷ S. E. Kuhlmann,² K. Kurino,¹⁷ T. Kuwabara,⁴³ A. T. Laasanen,³⁶ N. Lai,⁸ S. Lami,³⁸ S. Lammel,¹¹ J. I. Lamoureux,⁴ J. Lancaster,¹⁰ M. Lancaster,²³ R. Lander,⁵ G. Latino,³⁴ T. LeCompte,² A. M. Lee IV,¹⁰ K. Lee,⁴¹ S. Leone,³⁴ J. D. Lewis,¹¹ M. Lindgren,⁶ T. M. Liss,¹⁸ J. B. Liu,³⁷ Y. C. Liu,¹ N. Lockyer,³³ J. Loken,³¹ M. Loreti,³² D. Lucchesi,³² P. Lukens,¹¹ S. Lusin,⁴⁶ L. Lyons,³¹ J. Lys,²³ R. Madrak,¹⁶ K. Maeshima,¹¹ P. Maksimovic,¹⁶ L. Malferrari,³ M. Mangano,³⁴ M. Mariotti,³² G. Martignon,³² A. Martin,⁴⁷ J. A. J. Matthews,^{2,8} J. Mayer,²⁵ P. Mazzanti,³ K. S. McFarland,³⁷ P. McIntyre,⁴⁰ E. McKigney,³³ M. Menguzzato,³² A. Menzione,³⁴ C. Mesropian,³⁸ A. Meyer,¹¹ T. Miao,¹¹ R. Miller,²⁷ J. S. Miller,²⁶ H. Minato,⁴³ S. Miscetti,¹³ M. Mishina,²² G. Mitselmakher,¹² N. Moggi,³ E. Moore,²⁸ R. Moore,²⁶ Y. Morita,²² T. Moulik,²⁴ M. Mulhearn,²⁴ A. Mukherjee,¹¹ T. Muller,²⁰ A. Munar,³⁴ P. Murat,¹¹ S. Murgia,²⁷ J. Nachtman,⁶ S. Nahn,⁴⁷ H. Nakada,⁴³ T. Nakaya,⁸ I. Nakano,¹⁷ C. Nelson,¹¹ T. Nelson,¹¹ C. Neu,²⁹ D. Neuberger,²⁰ C. Newman-Holmes,¹¹ C.-Y. P. Ngan,²⁴ H. Niu,⁴ L. Nodulman,² A. Nomerotski,¹² S. H. Oh,¹⁰ T. Ohmoto,¹⁷ T. Ohsugi,¹⁷ R. Oishi,⁴³ T. Okusawa,³⁰ J. Olsen,⁴⁶ W. Orejudos,²³ C. Pagliarone,³⁴ F. Palmonari,³⁴ R. Paoletti,³⁴ V. Papadimitriou,⁴¹ S. P. Pappas,⁴⁷ D. Partos,⁴ J. Patrick,¹¹ G. Pauletta,⁴² M. Paulini,^{23,*} C. Paus,²⁴ L. Pescara,³² T. J. Phillips,¹⁰ G. Piacentino,³⁴ K. T. Pitts,¹⁸ A. Pompos,³⁶ L. Pondrom,⁴⁶ G. Pope,³⁵ M. Popovic,²⁵ F. Prokoshin,⁹ J. Proudfoot,² F. Ptohos,¹³ O. Pukhov,⁹ G. Punzi,³⁴ K. Ragan,²⁵ A. Rakitine,²⁴ D. Reher,²³ A. Reichold,³¹ A. Ribon,³² W. Riegler,¹⁶ F. Rimondi,³ L. Ristori,³⁴ M. Rivelino,²⁵ W. J. Robertson,¹⁰ A. Robinson,²⁵ T. Rodrigo,⁷ S. Rolli,⁴⁴ L. Rosenson,²⁴ R. Roser,¹¹ R. Rossin,³² A. Roy,²⁴ A. Safonov,³⁸ R. St. Denis,¹⁵ W. K. Sakumoto,³⁷ D. Saltzberg,⁶ C. Sanchez,²⁹ A. Sansoni,¹³ L. Santi,⁴² H. Sato,⁴³ P. Savard,²⁵ P. Schlabach,¹¹ E. E. Schmidt,¹¹ M. P. Schmidt,⁴⁷ M. Schmitt,¹⁶ L. Scodellaro,³² A. Scott,⁶ A. Scribano,³⁴ S. Segler,¹¹ S. Seidel,²⁸ Y. Seiya,⁴³ A. Semenov,⁹ F. Semeria,³ T. Shah,²⁴ M. D. Shapiro,²³ P. F. Shepard,³⁵ T. Shibayama,⁴³ M. Shimojima,⁴³ M. Shochet,⁸ J. Siegrist,²³ G. Signorelli,³⁴ A. Sill,⁴¹ P. Sinervo,²⁵ P. Singh,¹⁸ A. J. Slaughter,⁴⁷ K. Sliwa,⁴⁴ C. Smith,¹⁹ F. D. Snider,¹¹ A. Solodsky,³⁸ J. Spalding,¹¹ T. Speer,¹⁴ P. Sphicas,²⁴ F. Spinella,³⁴ M. Spiropulu,¹⁶ L. Spiegel,¹¹

J. Steele,⁴⁶ A. Stefanini,³⁴ J. Strologas,¹⁸ F. Strumia,¹⁴ D. Stuart,¹¹ K. Sumorok,²⁴ T. Suzuki,⁴³ T. Takano,³⁰
 R. Takashima,¹⁷ K. Takikawa,⁴³ P. Tamburello,¹⁰ M. Tanaka,⁴³ B. Tannenbaum,⁶ W. Taylor,²⁵ M. Tecchio,²⁶
 P. K. Teng,¹ K. Terashi,³⁸ S. Tether,²⁴ A. S. Thompson,¹⁵ R. Thurman-Keup,² P. Tipton,³⁷ S. Tkaczyk,¹¹ K. Tollefson,³⁷
 A. Tollestrup,¹¹ H. Toyoda,³⁰ W. Trischuk,²⁵ J. F. de Troconiz,¹⁶ J. Tseng,²⁴ N. Turini,³⁴ F. Ukegawa,⁴³ T. Vaiculis,³⁷
 J. Valls,³⁹ S. Vejcek III,¹¹ G. Velev,¹¹ R. Vidal,¹¹ R. Vilar,⁷ I. Volobouev,²³ D. Vucinic,²⁴ R. G. Wagner,² R. L. Wagner,¹¹
 J. Wahl,⁸ N. B. Wallace,³⁹ A. M. Walsh,³⁹ C. Wang,¹⁰ M. J. Wang,¹ T. Watanabe,⁴³ D. Waters,³¹ T. Watts,³⁹ R. Webb,⁴⁰
 H. Wenzel,²⁰ W. C. Wester III,¹¹ A. B. Wicklund,² E. Wicklund,¹¹ T. Wilkes,⁵ H. H. Williams,³³ P. Wilson,¹¹
 B. L. Winer,²⁹ D. Winn,²⁶ S. Wolbers,¹¹ D. Wolinski,²⁶ J. Wolinski,²⁷ S. Wolinski,²⁶ S. Worm,²⁸ X. Wu,¹⁴
 J. Wyss,³⁴ A. Yagil,¹¹ W. Yao,²³ G. P. Yeh,¹¹ P. Yeh,¹ J. Yoh,¹¹ C. Yosef,²⁷ T. Yoshida,³⁰ I. Yu,²¹ S. Yu,³³ Z. Yu,⁴⁷
 A. Zanetti,⁴² F. Zetti,²³ and S. Zucchelli³
 (CDF Collaboration)

¹*Institute of Physics, Academia Sinica, Taipei, Taiwan 11529, Republic of China*

²*Argonne National Laboratory, Argonne, Illinois 60439*

³*Istituto Nazionale di Fisica Nucleare, University of Bologna, I-40127 Bologna, Italy*

⁴*Brandeis University, Waltham, Massachusetts 02254*

⁵*University of California at Davis, Davis, California 95616*

⁶*University of California at Los Angeles, Los Angeles, California 90024*

⁷*Instituto de Fisica de Cantabria, CSIC-University of Cantabria, 39005 Santander, Spain*

⁸*Enrico Fermi Institute, University of Chicago, Chicago, Illinois 60637*

⁹*Joint Institute for Nuclear Research, RU-141980 Dubna, Russia*

¹⁰*Duke University, Durham, North Carolina 27708*

¹¹*Fermi National Accelerator Laboratory, Batavia, Illinois 60510*

¹²*University of Florida, Gainesville, Florida 32611*

¹³*Laboratori Nazionali di Frascati, Istituto Nazionale di Fisica Nucleare, I-00044 Frascati, Italy*

¹⁴*University of Geneva, CH-1211 Geneva 4, Switzerland*

¹⁵*Glasgow University, Glasgow G12 8QQ, United Kingdom*

¹⁶*Harvard University, Cambridge, Massachusetts 02138*

¹⁷*Hiroshima University, Higashi-Hiroshima 724, Japan*

¹⁸*University of Illinois, Urbana, Illinois 61801*

¹⁹*The Johns Hopkins University, Baltimore, Maryland 21218*

²⁰*Institut für Experimentelle Kernphysik, Universität Karlsruhe, 76128 Karlsruhe, Germany*

²¹*Center for High Energy Physics, Kyungpook National University, Taegu 702-701, Korea,
 Seoul National University, Seoul 151-742, Korea,
 and SungKyunKwan University, Suwon 440-746, Korea*

²²*High Energy Accelerator Research Organization (KEK), Tsukuba, Ibaraki 305, Japan*

²³*Ernest Orlando Lawrence Berkeley National Laboratory, Berkeley, California 94720*

²⁴*Massachusetts Institute of Technology, Cambridge, Massachusetts 02139*

²⁵*Institute of Particle Physics, McGill University, Montreal H3A 2T8, Canada*

and University of Toronto, Toronto M5S 1A7, Canada

²⁶*University of Michigan, Ann Arbor, Michigan 48109*

²⁷*Michigan State University, East Lansing, Michigan 48824*

²⁸*University of New Mexico, Albuquerque, New Mexico 87131*

²⁹*The Ohio State University, Columbus, Ohio 43210*

³⁰*Osaka City University, Osaka 588, Japan*

³¹*University of Oxford, Oxford OX1 3RH, United Kingdom*

³²*Universita di Padova, Istituto Nazionale di Fisica Nucleare, Sezione di Padova, I-35131 Padova, Italy*

³³*University of Pennsylvania, Philadelphia, Pennsylvania 19104*

³⁴*Istituto Nazionale di Fisica Nucleare, University and Scuola Normale Superiore of Pisa, I-56100 Pisa, Italy*

³⁵*University of Pittsburgh, Pittsburgh, Pennsylvania 15260*

³⁶*Purdue University, West Lafayette, Indiana 47907*

³⁷*University of Rochester, Rochester, New York 14627*

³⁸*Rockefeller University, New York, New York 10021*

³⁹*Rutgers University, Piscataway, New Jersey 08855*

⁴⁰*Texas A&M University, College Station, Texas 77843*

⁴¹*Texas Tech University, Lubbock, Texas 79409*

⁴²*Istituto Nazionale di Fisica Nucleare, University of Trieste/ Udine, Italy*

⁴³*University of Tsukuba, Tsukuba, Ibaraki 305, Japan*

⁴⁴*Tufts University, Medford, Massachusetts 02155*

⁴⁵*Waseda University, Tokyo 169, Japan*

⁴⁶*University of Wisconsin, Madison, Wisconsin 53706*⁴⁷*Yale University, New Haven, Connecticut 06520*

(Received 12 May 2000; published 20 August 2001)

We have measured the p_T distribution of top quarks that are pair produced in $p\bar{p}$ collisions at $\sqrt{s} = 1.8$ TeV using a sample of $t\bar{t}$ decays in which we observe a single high- p_T charged lepton, a neutrino, and four or more jets. We use a likelihood technique that corrects for the experimental bias introduced due to event reconstruction and detector resolution effects. The observed distribution is consistent with the standard model prediction. We use these data to place limits on the production of high- p_T top quarks suggested in some models of anomalous top quark pair production.

DOI: 10.1103/PhysRevLett.87.102001

PACS numbers: 14.65.Ha, 13.85.Ni, 13.85.Qk

The existence of the top quark has now been established [1–3]. In the standard model, the dominant mechanism for top quark production at the Fermilab Tevatron $p\bar{p}$ Collider is quark-antiquark pair production. However, a number of theoretical investigations [4] have concluded that alternative production mechanisms may play an important role in top production at the Tevatron. In many cases, the kinematic distributions associated with top quark pair production can be significantly modified, so measurement of these distributions can be a sensitive probe of these non-standard model phenomena. In particular, many exotic models predict sizable enhancements in the cross section for the production of top quarks having transverse momentum $p_T > 200$ GeV/ c . This Letter describes the first extraction of the true top quark p_T distribution and provides limits on high- p_T top quark production. Previous studies [5] compared the measured top quark p_T with standard model predictions and did not include an extraction of the true top quark p_T distribution that could be compared with other theoretical models.

In this analysis, we use a sample of $t\bar{t}$ candidates produced in $p\bar{p}$ collisions at $\sqrt{s} = 1.8$ TeV and detected with the Collider Detector at Fermilab (CDF). The integrated luminosity of our data sample is 106 pb^{-1} . In the standard model, the top quark decays predominantly to a final state consisting of a W boson and a b quark. We consider those $t\bar{t}$ final states, where one of the resulting W bosons decays leptonically into either an $e\bar{\nu}_e$ or $\mu\bar{\nu}_\mu$ pair while the other W boson in the event decays hadronically. This final state and its charge conjugate are known as the “lepton + jets” channel and provide a statistically significant measurement of various $t\bar{t}$ kinematic distributions.

The Collider Detector at Fermilab is a multipurpose detector, equipped with a charged particle spectrometer incorporating a 1.4 T magnetic field and a finely segmented calorimeter. As particles move outwards from the interaction region, they encounter different detector subsystems that are described in detail elsewhere [6]. Closest to the beam pipe is a silicon vertex detector (SVX). The SVX allows for precise track reconstruction in the transverse plane, and allows for reconstruction of secondary vertices from heavy flavor decays. The momenta of charged particles are measured outside the SVX in an 84-layer drift chamber that extends to a radius of 1.3 m. Outside the tracking system, electromagnetic and hadronic calorime-

ters in the pseudorapidity [7] region $|\eta| < 4.2$ are used to identify jets and electron candidates. The calorimeters also provide a measurement of the missing transverse energy \cancel{E}_T [8], which can be related to the net transverse energy associated with neutrinos in the final state. In the region $|\eta| < 1.0$ outside the calorimeters, drift chambers provide muon identification. A three-level trigger selects in real time the electron and muon candidates used in this analysis [1].

The data samples for this analysis are subsets of inclusive lepton events that contain an isolated electron with $E_T > 20$ GeV or an isolated muon with $p_T > 20$ GeV/ c . After the removal of Z boson candidates by rejecting events with two opposite-sign candidate leptons with invariant mass between 75 and 105 GeV/ c^2 , an inclusive W data sample is made by requiring $\cancel{E}_T > 20$ GeV. We further require that there be at least three jets in the event satisfying the “tight” selection requirements $E_T > 15$ GeV and $|\eta| < 2.0$. This results in a sample of 324 events. In order to ensure that the kinematics of the event are constrained by the measured jet energies, we demand that there be a fourth jet in the event, satisfying the less stringent requirements $E_T > 8$ GeV and $|\eta| < 2.4$. Finally, to increase the signal significance, we demand that either the lowest E_T jet satisfy the tight jet cuts or that at least one jet be associated with a b -quark decay. Two so-called “ b -tagging” methodologies are employed to identify such jets, both of which are described in [2]. Eighty-three events pass these selection criteria, 34 of which possess b -tagged jets.

In order to reconstruct the events, we employ a kinematic fit similar to that used in the measurement of the top quark mass [9]. As opposed to using this fit to measure the top quark mass, we constrain the top quark mass to $175 \text{ GeV}/c^2$, a value close to the world average measurement of this quantity [10].

We reject events having $\chi^2 > 10$ in this three-constraint kinematic fit, leaving 61 events in the data sample. We estimate using a Monte Carlo calculation showing that, after this cut is applied, the fraction of $t\bar{t}$ events for which the correct jet-parton assignment is made is approximately 30% for events possessing no b tags, 40% for events possessing a single b -tagged jet, and 60% for events possessing two b -tagged jets. In events for which the incorrect jet-parton assignment is made, there exists only a weak correlation between the measured and true p_T . In

Fig. 1 the distribution of reconstructed top quark momenta in HERWIG [11] Monte Carlo samples for top quarks having true p_T 's in four different ranges between 0 and 300 GeV/c is depicted. The Monte Carlo calculation that is used to construct these curves, which we shall refer to as our "response functions," includes a simulation of the effects introduced by our reconstruction algorithm and the resolution of the CDF detector. There is a strong correlation between the measured p_T 's for the top and anti-top quarks in a given event. Because of this correlation, we perform our measurement of the p_T spectrum using only the fully reconstructed hadronic top quark decay candidates.

The estimate of the background level in the candidate sample is based on the calculation performed in our measurement of the $t\bar{t}$ production cross section [12]. We correct for differences in the selection criteria between the cross section measurement and the present analysis. The estimated background contribution is 31.9 ± 4.6 events. Events arising from $W + \text{jets}$ production are estimated to make up approximately 70% of this background contribution while 20% is expected to originate from QCD multijet production, where one jet is misidentified as a lepton [13]. The remaining background comes from a variety of smaller sources such as single top and $Z + \text{jets}$ production. We estimate the shape of the background p_T distribution, $V(p_T)$, using a VECBOS Monte Carlo calculation.

The distribution of measured p_T for the 61 events is shown in Fig. 2. To correct for the p_T bias due to the

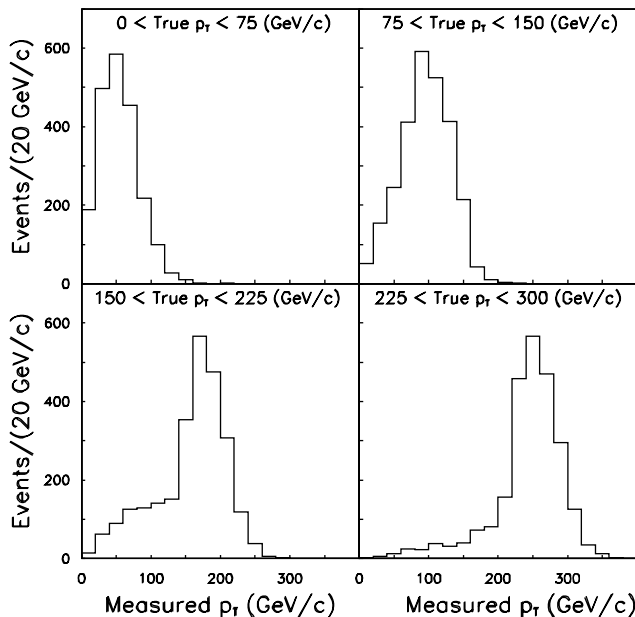


FIG. 1. The reconstructed p_T distribution in each of four true p_T bins for Monte Carlo $t\bar{t}$ events. These curves include a simulation of the resolution effects introduced by our reconstruction algorithm and the resolution of the CDF. The true p_T distribution within each bin is the HERWIG prediction. This plot includes only the hadronically decaying top quarks.

reconstruction and resolution effects illustrated in Fig. 1, we use an unsmearing procedure appropriate for small data samples. This procedure extracts the fraction of top quarks that are produced in each of four p_T bins of width 75 GeV/c, spanning the range between 0 and 300 GeV/c. We perform an unbinned likelihood fit to the measured p_T distribution, using a superposition of our response functions and the background template. The logarithm of the likelihood function that we maximize is

$$\ln[\mathcal{L}] = \sum_{i=1}^{n_{\text{data}}} \left\{ \ln \left[\sum_{j=1}^{n_{\text{bin}}} [(1-B)R_j T_j(p_T^i)] + BV(p_T^i) \right] \right\} - \frac{(B - \mu_b)^2}{2\sigma^2(\mu_b)}. \quad (1)$$

In this equation, R_j is the fitted fraction of top quarks produced in true bin j , while the $T_j(p_T)$ are the response functions for the $t\bar{t}$ signal and $V(p_T)$ is the background template. The fit parameter B is the fitted background fraction and $\mu_b \pm \sigma(\mu_b)$ is the estimated background fraction. We separate the data into two "tagging subsamples," one of which consists of the subset of events with one or more b tags, the other consisting of those events with no b tags. We fit the subsamples with and without b tags by using forms for the response functions, $T_j(p_T)$, appropriate for the subsample under consideration.

The response functions $T_j(p_T)$ depend on the form of the true p_T distribution within each p_T bin. Thus, we employ an iterative technique that interpolates the true p_T distribution across a given bin based upon the current R_i parameter values. The iteration begins with R_i values equal to the fraction of observed events in each p_T bin and determines a new set of R_i values and a modified set of response functions. A linear variation within each bin is assumed, and we constrain the true p_T spectrum to go to zero for $p_T = 0$.

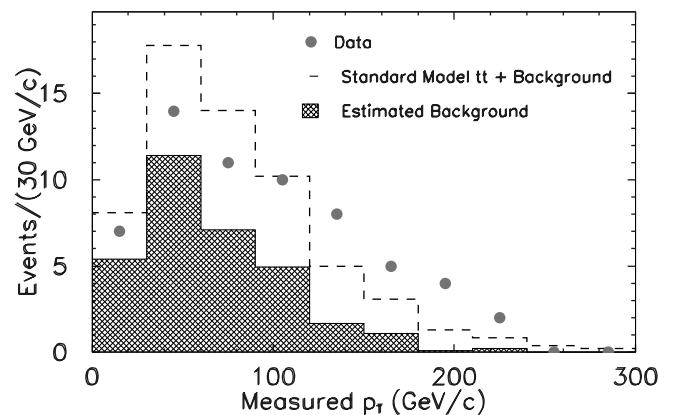


FIG. 2. The measured p_T distribution for the hadronically decaying top quarks in the 61-event sample. The hatched distribution is the estimated background distribution, normalized to the estimated number of background events. The dashed distribution is the standard model prediction, normalized to the observed number of candidate events.

TABLE I. A summary of the systematic uncertainties. The magnitudes of these uncertainties have been estimated using the means of each measured variable in Monte Carlo pseudoexperiments. These uncertainties have not been scaled by the acceptance correction.

Systematic Effect	δR_1	δR_2	δR_3	δR_4	$\delta(R_1 + R_2)$
Top quark mass	+0.026 -0.008	+0.000 -0.035	+0.039 -0.000	+0.000 -0.018	+0.010 -0.020
Initial state radiation	± 0.021	± 0.012	± 0.011	± 0.009	± 0.011
Final state radiation	± 0.037	± 0.022	± 0.009	± 0.005	± 0.015
Jet energy scale	+0.047 -0.020	+0.005 -0.043	+0.032 -0.000	+0.000 -0.016	+0.011 -0.023
Background model	± 0.025	± 0.008	± 0.008	± 0.010	± 0.017
Shape of p_T spectrum	± 0.037	± 0.027	± 0.051	± 0.021	± 0.045

We correct the resulting R_i fit values for the fact that the $t\bar{t}$ acceptance is a function of top quark p_T . The relative acceptance in each bin of true p_T is measured using our Monte Carlo calculation and detector simulation. Normalizing the acceptance in the lowest bin of true p_T to 1, the relative acceptance in the subsequent three p_T bins is 1.16 ± 0.01 , 1.34 ± 0.02 , and 1.24 ± 0.04 , where the uncertainties are statistical only.

An important systematic uncertainty in our measurement is associated with the effect of varying the shape of the true p_T distribution within each bin. We estimate the systematic uncertainty arising from this source by measuring the residual bias that remains after the unsmearing is performed. This quantity is estimated by comparing the means of the outcomes of a large number of Monte Carlo “pseudoexperiments” with the expected values for the four R_i ’s, making various assumptions for the true p_T distribution. We considered a variety of different true p_T distributions. These include distributions that peak at p_T values between 50 and 200 GeV/ c , and distributions whose forms were inspired by Ref. [4]. The largest bias observed for each R_i is taken as a symmetric systematic uncertainty for this parameter. The results of this calculation are shown in Table I.

We estimate the remaining systematic uncertainties, also presented in Table I, using a similar procedure, but where both the response functions and the Monte Carlo pseudoexperiments are generated by assuming the standard model p_T distribution. Since we constrain the top quark mass to 175 GeV/ c^2 , we vary the top quark mass between 170 and 180 GeV [10] and take the largest variation in the means of the R_i for our pseudoexperiments as a systematic uncertainty. Similarly, we estimate the contribution of initial and final state radiation by varying the level of QCD

radiation predicted by the Monte Carlo calculation. We do this using the PYTHIA Monte Carlo simulation [14] of standard model $t\bar{t}$ production, as this calculation allows us to readily manipulate the expected QCD radiation within the constraints set by the observed jet multiplicity distribution. We estimate the systematic uncertainty due to our modeling of the background by varying the Q^2 scale in the VECBOS $W + \text{jets}$ Monte Carlo calculation [15] from M_W^2 to $\langle p_T \rangle^2$. Finally, we measure a systematic uncertainty in the acceptance corrections by computing the change in relative acceptance induced by the variation of each of the systematic effects detailed above.

The resulting values for the four R_i are compared to the standard model prediction in Table II. We also show the result for $R_1 + R_2$, the fraction of top quarks that are produced with $p_T < 150$ GeV/ c (due to a strong negative correlation between the fitted values of R_1 and R_2 , the fractional uncertainty in this result is much smaller than it is for the individual estimates for R_1 and R_2). The standard model predictions are calculated using the HERWIG Monte Carlo generator and the MRSD0’ parton distribution functions [16]. We have also performed a Kolmogorov-Smirnov test for compatibility between the standard model prediction and the reconstructed p_T distribution depicted in Fig. 2. Assuming our default Monte Carlo calculation to be correct, the probability to observe a difference between the two distributions as large as the one that is measured is calculated to be 5.0%. This probability varies between 1.0% and 9.4% when the background level and each of the systematic effects are varied by one standard deviation in our model.

We also calculated a 95% confidence level upper limit on R_4 by combining the statistical and systematic uncertainties using a convolution of the likelihood function for

TABLE II. The results of our measurement of the top quark p_T distribution. The standard model expectation is generated by using the HERWIG Monte Carlo program.

p_T Bin	Parameter	Measurement	Standard Model Expectation
$0 \leq p_T < 75$ GeV/ c	R_1	$0.21^{+0.22}_{-0.21}(\text{stat})^{+0.10}_{-0.08}(\text{syst})$	0.41
$75 \leq p_T < 150$ GeV/ c	R_2	$0.45^{+0.23}_{-0.23}(\text{stat})^{+0.04}_{-0.07}(\text{syst})$	0.43
$150 \leq p_T < 225$ GeV/ c	R_3	$0.34^{+0.14}_{-0.12}(\text{stat})^{+0.07}_{-0.05}(\text{syst})$	0.13
$225 \leq p_T < 300$ GeV/ c	R_4	$0.000^{+0.031}_{-0.000}(\text{stat})^{+0.024}_{-0.000}(\text{syst})$	0.025
$0 \leq p_T < 150$ GeV/ c	$R_1 + R_2$	$0.66^{+0.17}_{-0.17}(\text{stat})^{+0.07}_{-0.07}(\text{syst})$	0.84

R_4 with a Gaussian distribution, G , that represents the systematic uncertainties. The result of this calculation is

$$R_4 < 0.16 \text{ at } 95\% \text{ C.L.} \quad (2)$$

This limit was calculated using the same iterative technique that was used to estimate the four R_i 's from the data. This methodology has been shown to produce unbiased results for a wide variety of signal distributions, including those predicted by a number of models [4] of top quark production [17].

We also searched for top quark production with true $p_T > 300 \text{ GeV}/c$ by modifying our final response function to incorporate a possible high- p_T component and subsequently recalculating our upper limit. Since the largest limit is obtained by assuming no high- p_T component, we conclude that our upper limit can be extended into a conservative upper limit on the fraction of top quarks produced with p_T in the range 225–425 GeV/c . Above this p_T value, we find our relative acceptance for top quarks to begin to fall, reducing to 50% of the acceptance at 225 GeV/c for top quarks produced with $p_T = 500 \text{ GeV}/c$.

In summary, we have made the first measurement of the true top quark p_T distribution. We have also computed a 95% confidence level upper limit on the fraction of top quarks that are produced with $225 < p_T < 425 \text{ GeV}/c$, and find that $R_4 < 0.16$ at 95% C.L.

We thank the Fermilab staff and the technical staffs at the participating institutions for their contributions. This work was supported by the U.S. Department of Energy and the National Science Foundation, the Italian Istituto Nazionale di Fisica Nucleare, the Ministry of Science, Culture and Education of Japan, the Natural Sciences and Engineering Research Council of Canada, the National Science Council of the Republic of China, and the A.P. Sloan Foundation.

*Present address: Carnegie Mellon University, Pittsburgh, Pennsylvania 15213.

- [1] CDF Collaboration, F. Abe *et al.*, Phys. Rev. D **50**, 2966 (1994).
- [2] CDF Collaboration, F. Abe *et al.*, Phys. Rev. Lett. **74**, 2626 (1995).
- [3] D0 Collaboration, S. Abachi *et al.*, Phys. Rev. Lett. **74**, 2632 (1995).
- [4] C. T. Hill and S. J. Parke, Phys. Rev. D **49**, 4454 (1994); T. G. Rizzo, hep-ph/9902273; E. Simmons, hep-ph/9908511; K. Lane, Phys. Rev. D **52**, 1546 (1995).
- [5] D0 Collaboration, B. Abbott *et al.*, Phys. Rev. D **58**, 052001 (1998).
- [6] F. Abe *et al.*, Nucl. Instrum. Methods Phys. Res., Sect. A **271**, 387 (1988); D. Amidei *et al.*, Nucl. Instrum. Methods Phys. Res., Sect. A **350**, 73 (1994).
- [7] We denote by r the radial distance from the beam line and use θ and ϕ to symbolize the polar and azimuthal angles, respectively. The pseudorapidity, η , is defined as $-\ln[\tan(\theta/2)]$. The transverse momentum of a particle with momentum p is $p_T = p \sin\theta$. The transverse energy is $E_T = E \sin\theta$, where E is the particles energy as measured in the calorimeter.
- [8] The missing transverse energy, $\vec{\cancel{E}}_T$ is defined to be $-\sum_i E_T^i \hat{n}_i$, where \hat{n}_i is a unit vector in the azimuthal plane pointing from the beam line to calorimeter tower i .
- [9] CDF Collaboration, F. Abe *et al.*, Phys. Rev. Lett. **80**, 2767 (1998).
- [10] Particle Data Group, C. Caso *et al.*, Eur. Phys. J. C **3**, 1 (1998).
- [11] G. Marchesini and B.R. Webber, Nucl. Phys. **B310**, 461 (1998); G. Marchesini *et al.*, Comput. Phys. Commun. **67**, 465 (1992). We use HERWIG version 5.6.
- [12] CDF Collaboration, T. Affolder *et al.*, Report No. FERMILAB-PUB-01-007-E (to be published). CDF Collaboration, F. Abe *et al.*, Phys. Rev. Lett. **80**, 2779 (1998).
- [13] CDF Collaboration, T. Affolder *et al.*, Phys. Rev. D **63**, 011101 (2001).
- [14] T. Sjöstrand, Comput. Phys. Commun. **82**, 74 (1994).
- [15] F.A. Berends, W.T. Giele, H. Kujif, and B. Tausk, Nucl. Phys. **B357**, 32 (1991).
- [16] A.D. Martin, R.G. Roberts, and W.J. Stirling, Phys. Lett. B **308**, 145 (1993).
- [17] This methodology does result in a small bias for those signal distributions that concentrate in excess of 80% of the events within the final true p_T bin close to 225 GeV/c . If we allow such nonphysical distributions to be candidate theories, the 95% C.L. limit on R_4 rises to 0.19.